ELSEVIER

Applied Catalysis A: General 215 (2001) 39–45

APPLIED CATALYSIS A: GENERAL

www.elsevier.com/locate/apcata

Characterization and catalytic properties of supported nickel molybdenum nitrides for hydrodenitrogenation

Wang Yuhong, Li Wei, Zhang Minghui, Guan Naijia, Tao Keyi*

Institute of New Catalytic Material Science, Department of Chemistry, Nankai University, Tianjin 300071, PR China

Received 5 October 2000; received in revised form 17 January 2001; accepted 25 January 2001

Abstract

The characterization and hydrodenitrogenation activity of 3-methyl pyridine have been obtained. The results from the characterization techniques (X-ray diffraction (XRD), temperature-programmed reaction (TPR) and XPS) were used to illustrate the structure, surface reduction properties and the role of Ni metal in the reaction. The $NiMoN_x/\gamma\text{-}Al_2O_3$ catalyst is more active than a $Mo_2N/\gamma\text{-}Al_2O_3$ catalyst with the same MoO_3 loading. Mo_2N, Ni_3Mo_3N and Ni metal are formed in the $NiMoN_x/\gamma\text{-}Al_2O_3$ catalyst; moreover, the synergy among them is probably responsible for the high activity of $NiMoN_x/\gamma\text{-}Al_2O_3$ catalyst. The addition of Ni metal enhances the reducibility of $Mo_2N/\gamma\text{-}Al_2O_3$ phase and also promotes the HDN activity. The reasons for reduction before reaction and the surface ion state changes during reduction are illustrated by XPS techniques.

Keywords: XRD; TPR; XPS; $NiMoN_x/\gamma\text{-}Al_2O_3$; HDN; 3-Methyl pyridine

1. Introduction

Because high specific surface area early transition metal nitrides, prepared using a topotactic reaction method, exhibit catalytic properties similar to group VIII metals [1], they have attracted attention for a number of catalytic reactions and have demonstrated strong potential for use in the hydrodenitrogenation (HDN) [2].

Unsupported and supported Mo_2N have been tested for HDN reactions, using some individual model compounds, such as indole [3] and quinoline [4], and also with complex feedstock [5]. Much higher activity of nitride catalyst compared with a sulfide $NiMo/\gamma\text{-}Al_2O_3$ catalyst was reported.

However, most studies focused on monometallic transition metal nitrides; relatively few bimetallic compounds have been synthesized and fully characterized. Recently, bimetallic VMo oxynitride catalyst has been prepared. Its HDN catalytic activity was higher than those of the pure compounds VN, Mo_2N and a commercial sulfide $NiMo/\gamma\text{-}Al_2O_3$ catalyst in terms of the number of metal active sites [6].

Nickel has been used as an effective promoter in sulfide $Mo/\gamma\text{-}Al_2O_3$ catalysts for hydrotreating process, but there is little study on the promotion effect of nickel in molybdenum nitride catalyst. In the current investigation, $NiMoN_x/\gamma\text{-}Al_2O_3$ catalyst was synthesized by a temperature-programmed reaction (TPR) using a bimetallic oxide $NiO{\cdot}MoO_3/\gamma\text{-}Al_2O_3$ as the precursor. Several characterization techniques, including X-ray diffraction (XRD), TPR and XPS, explained the structure, reducibility and surface ion state changes during reduction on the catalyst surface. Furthermore,

* Corresponding author. Tel.: +86-22-23500027; fax: +86-22-23500027.
E-mail address: kytao@263.net (T. Keyi).

0926-860X/01/$ – see front matter
PII: S0926-860X(01)00537-3

the reactivity in 3-methyl pyridine HDN at 3.0 MPa total pressure was studied carefully and the results were compared with those of the corresponding monometallic nitrides, $Mo_2N/\gamma\text{-}Al_2O_3$.

2. Experimental

2.1. Catalyst synthesis

The details concerning the preparation and passivation of $Mo_2N/\gamma\text{-}Al_2O_3$ and $NiMoN_x/\gamma\text{-}Al_2O_3$ have been described elsewhere [7,8]. In brief, $MoO_3/\gamma\text{-}Al_2O_3$ and $NiO{\cdot}MoO_3/\gamma\text{-}Al_2O_3$ were prepared using an incipient impregnation method and nitrides were synthesized by the TPR of precursors in NH_3 flow.

$MoO_3/\gamma\text{-}Al_2O_3$ precursors were prepared by impregnation of precalcined (773 K, 5 h, dry air) $\gamma\text{-}Al_2O_3$ with aqueous solutions of ammonium heptamolybdate ($(NH_4)_6Mo_7O_{24}{\cdot}4H_2O$), followed by drying for 3 h at 393 K and calcination for 5 h at 773 K in air.

A series of $NiO{\cdot}MoO_3/\gamma\text{-}Al_2O_3$ precursors were prepared using a coimpregnation method. The aqueous solution of ammonium heptamolybdate ($(NH_4)_6Mo_7O_{24}{\cdot}4H_2O$) and nickel nitrate ($Ni(NO_3)_2{\cdot}6H_2O$) were added at room temperature to precalcined (773 K, 5 h, dry air) $\gamma\text{-}Al_2O_3$. The solution was filtered and the resulting cakes were then dried at 393 K for 3 h and calcined at 773 K for 5 h in dry air.

Nitrides were prepared by TPR of the oxide precursors in a reactant gas stream (NH_3). A typical synthesis consisted of loading about 6 ml of the oxide precursor in a quartz reactor placed in a tubular furnace. A temperature programmer controller controlled the temperature of the furnace. A thermocouple placed in a thermocouple well located close to the reactor bed measured the temperature of the bed. The flowing ammonia was at a volume VHSV of about 7500 h^{-1}. The temperature was increased in three steps: first rapidly from room temperature to 623 K (30 min), then more slowly from 623 to 723 K (1 K/min), and finally from 723 to 973 K (2.5 K/min). The temperature was held at 973 K for 2 h. The system was then cooled to RT in flowing NH_3 and passivated by flowing 1% O_2/He (v/v) to avoid a strong bulk oxidation.

For supported NiO and MoO_3 samples, when the loading of MoO_3 and NiO is lower than 15 and 5.0 wt.%, respectively, the patterns of XRD cannot be discerned. Therefore, several high loading oxide precursors: 30 wt.% $MoO_3/\gamma\text{-}Al_2O_3$, 15 wt.% $NiO/\gamma\text{-}Al_2O_3$, and 15 wt.% NiO, 30 wt.% $MoO_3/\gamma\text{-}Al_2O_3$, were prepared for XRD measurement. The other preparation processes were the same as described above.

2.2. X-ray diffraction (XRD)

The crystalline structures were determined using XRD. The XRD patterns of the samples were taken on a D/max-2500 power X-ray diffractometer (Cu Kα radiation). Data acquisition, peak identification, and data plotting were accomplished using a Data General computer system.

2.3. H_2-temperature-programmed reduction (H_2-TPR)

A 10 mg sample in a quartz reactor was purged with N_2 at 773 K for 1 h in order to remove some adsorbed NH_x species and other impurities on the surface of the sample. After the sample was cooled to room temperature in flowing N_2, TPR was carried out in 10% H_2/N_2 (v/v) mixture with a flowing rate of 60 ml/min. The heating rate was 12 K/min from room temperature to 823 K; after soaking at 823 K for 1 h, TPR profiles were recorded with a thermal conductivity detector.

2.4. X-ray photoelectron spectroscopy (XPS)

A PHI5300 apparatus at Shell KSLA was used for X-ray photoelectron analysis using an Al Kα monochromatized radiation source. As the N 1s and Mo $3p_{3/2}$ signals overlapped, the nitrogen present on the surface has been estimated by integration of the N signal at ca.1000 eV. Integration of the O 1s signal was used to calculate the amount of superficial oxygen. Mo(IV) and Mo(VI) ratios were calculated by deconvolution of the Mo $3d_{3/2}$ and $3d_{5/2}$ signals.

2.5. Catalytic properties

The catalytic properties were measured with 5 ml catalyst (20/40 mesh). The reaction was operated under 3.0 MPa. A stream of 10% 3-methyl pyridine introduced by a liquid feedstock pump in H_2 flowed

over the bed of catalyst particles. The flow rate of H_2 was maintained at 60 ml/min and the liquid flow rate was 5.0 ml/h. Prior to evaluation, the catalysts were heated to 673 K in flowing H_2; after being held at 673 K for 2 h, they were cooled to the reaction temperature. The reactor effluent was analyzed using a SP-502 gas chromatograph.

3. Results and discussion

3.1. XRD

Fig. 1 shows the XRD patterns of the Mo_2N/γ-Al_2O_3, NiN_x/γ-Al_2O_3, and $NiMoN_x$/γ-Al_2O_3 catalysts. The diffraction pattern for a 30 wt.% Mo_2N/γ-Al_2O_3 catalyst shows peaks at 36.2°, 44.2°, and 63.0°, which are assigned to the {1 1 1}, {2 0 0}, and {2 2 0} reflections of bulk γ-Mo_2N, respectively [9]. The other peaks at 45.8°, 67.1°, and 75.5° can be assigned to the γ-Al_2O_3 support. There were no peaks assigned to the unreacted Mo oxides or to other nitrides exclusive of γ-Mo_2N.

For NiN_x/γ-Al_2O_3 sample, the expected diffraction peaks of Ni_3N are not detected, while the peaks at $2\theta = 44.4°$ and 51.7° due to typical diffraction peaks of metallic Ni appear.

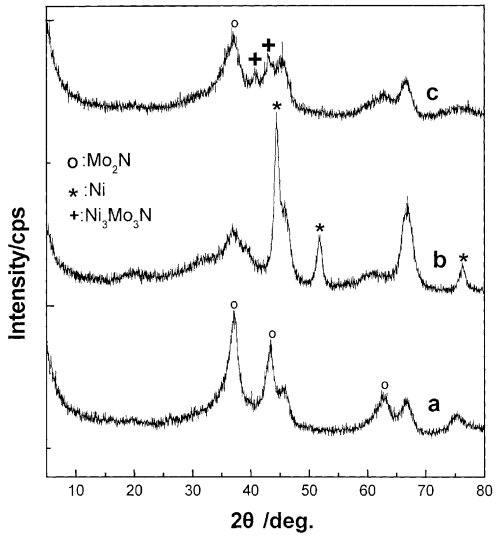

Fig. 1. XRD patterns of: (a) Mo_2N/γ-Al_2O_3; (b) NiN_x/γ-Al_2O_3; (c) $NiMoN_x$/γ-Al_2O_3.

With $NiMoN_x$/γ-Al_2O_3 catalyst, the peak at $2\theta = 39.8°$ attributed to γ-Mo_2N is found, but no diffraction peak of Ni emerges. Moreover, new peaks appear at $2\theta = 40.8°$ and 43.0°. It has been reported that the characteristic XRD peaks of Ni_3Mo_3N compound prepared similarly to nitride in this study are located at $2\theta = 40.8°$ and 43.0° [10]. Thus, these two peaks may be ascribed to Ni_3Mo_3N phase too. Although one of characteristic peaks of metallic Mo at $2\theta = 40.8°$ emerges, the other characteristic peak ($2\theta = 73.3°$) does not appear. Therefore, a new phase of Ni_3Mo_3N is formed on $NiMoN_x$/γ-Al_2O_3 in this study, and the species existing on the lower loaded $NiMoN_x$/γ-Al_2O_3 catalysts used in the HDN reaction are probably similar to those on the samples tested by the XRD.

3.2. H_2-TPR

For passivated nitride samples, only weakly adsorbed NH_x species are present, desorbed at 473–573 K. Above 800 K, a gradual bulk reduction occurs, but the destructive decomposition cannot be observed until higher temperature is reached. The H_2 consumption peak around 773 K for passivated nitride samples is attributed to the reduction of the passivating oxygen [11]. Fig. 2 shows the low temperature H_2-TPR profiles of supported nitride samples. For Mo_2N/γ-Al_2O_3, the peak begins at 563 K and maximizes at 803 K, due to the reduction of surface oxygen on passivated nitrided Mo. With increase in the amount of nickel added, the low temperature peak at 766 K shifts to lower temperature gradually. From the TPR profiles, it is obvious that the Ni added decreases the reduction temperature of the passivation layer of nitride.

3.3. XPS

Because $NiMoN_x$/γ-Al_2O_3 is a pyrophoric compound, a passivation step is necessary after nitridation to avoid bulk oxidation when contacting with air. However, passivated $NiMoN_x$/γ-Al_2O_3 nitrides have a high affinity for oxygen. Indeed, oxygen can be incorporated into the lattice of the nitrides during the passivation step [12]. The absorbed oxygen has a poisonous effect on the catalyst surface and an apparent loss of the specific surface area is observed during passivation [13,14]. So the materials need to suffer a reduction step to remove oxygen.

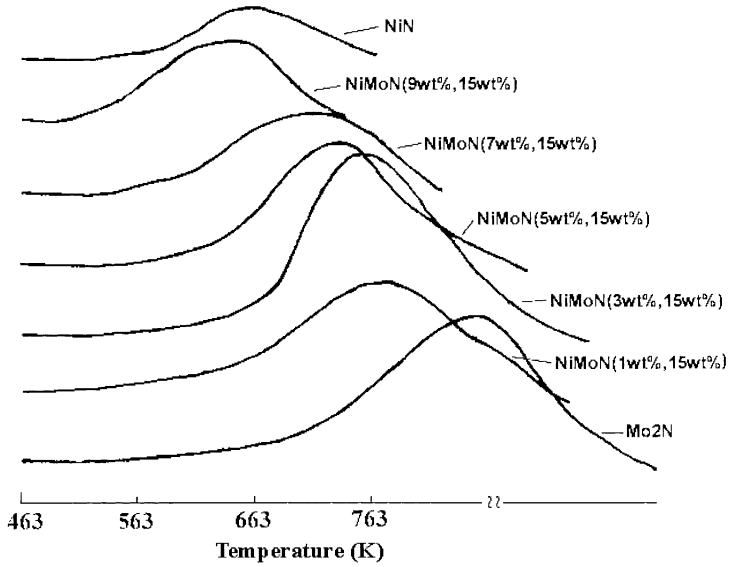

Fig. 2. TPR profiles; all samples were supported on γ-Al_2O_3.

Oxygen is incorporated into the samples during passivation. However, XRD data shows no evidence of crystalloid molybdenum oxide formation. Therefore, we conclude that passivation produces a protective, amorphous and surface oxide slightly greater than one-monolayer thick. Passivated $NiMoN_x/\gamma$-Al_2O_3 should be reduced by H_2 at moderate temperature in order to achieve high HDN activity.

The valence state and distribution of Mo ions can be known from Mo 3d XPS spectra, which show the energy level surface of passivated $NiMoN_x/\gamma$-Al_2O_3 reduced by H_2 at different temperatures for 3 h. The results presented in Table 1 show that Mo 3d spectrum can be drawn out into three peaks. It means that there are three state Mo ions on the catalyst surface. The binding energy 230.0 ± 0.2 and 227.8 ± 0.2 eV are assigned to Mo^{4+} and Mo^0, respectively [15], while the binding energy 228.6 eV of Mo $3d_{5/2}$ was assigned to Mo^{2+} by Goldwasser et al. [16] Therefore, the binding energies 232.3, 229.8 and 228.2 eV are assigned to Mo^{6+}, Mo^{4+} and $Mo^{\delta+}$ ($0 < \delta < 2$), respectively.

Table 1 shows that Mo^{6+} and Mo^{4+} are major components of the passivated $NiMoN_x/\gamma$-Al_2O_3. The atomic ratio of N/Mo is higher than that in the ball

Table 1
Influence of H_2 reduction temperature on the surface of $NiMoN_x/\gamma$-Al_2O_3 catalysts[a]

Reduction temperature (K)	Atomic ratio		BE (eV)		BE of Mo $3d_{5/2}$ and concentration (%)		
	N/Mo	O/M	N 1s	O 1s	Mo^{6+} (232.30, 235.39)	Mo^{4+} (229.74, 233.37)	$Mo^{\delta+}$ (228.30, 230.80)
Without reduction	2.60	2.00	397.3	531.2	42	18	40
RT	1.63	0.80	397.2	531.2	37	20	43
373	0.57	0.84	397.4	531.4	37	18	45
473	0.41	0.60	397.2	531.3	36	20	44
573	0.57	0.77	397.1	531.3	17	25	58
673	0.50	0.58	397.3	531.2	14	28	58
773	0.51	0.39	397.2	531.1	10	22	68

[a] $N/Mo = I(N\ 1s)\sigma(Mo\ 3p_{3/2})/I\ (Mo\ 3p_{3/2})\sigma(\ 1s)$, $O/Mo = I(O\ 1s)\sigma(Mo\ 3d)/I(Mo\ 3d)\sigma(O\ 1s)$. RT: room temperature.

which means the theoretic ratios of N/Mo in the MoN crystal because lots of NH_3 has been absorbed on the surface during preparation. When reduced at room temperature, the chemically absorbed NH_3 and weakly chemically absorbed oxygen are removed, so the ratios of N/Mo and O/Mo decrease strongly and Mo^{6+} decreases slightly. Because the absorbed NH_3 is eliminated fully by being reduced at 373–473 K, the content of Mo ions on the surface increases relatively. So the ratios of N/Mo and O/Mo decrease strongly, but the compositions of Mo ions are unchanged. When the temperature is beyond 573 K, the ratio of N/Mo approaches the lattice value 0.5 and remains unchanged, but the ratio O/Mo and the content of Mo^{6+} decrease considerably, while the content of $Mo^{\delta+}$ increases intensively. Such results show that water, produced by the reaction of chemically absorbed oxygen with H_2, begins to be removed from the surface. After reduction at 773 K, the ratio of O/Mo only decreases by 80%, that is, there is some oxygen, considered as lattice oxygen, which is hard to be eliminated by reduction.

3.4. HDN activities of Mo_2N/γ-Al_2O_3 and $NiMoN_x/\gamma$-Al_2O_3 catalysts

The dependence of 3-methyl pyridine conversion on temperature over Mo_2N/γ-Al_2O_3 catalysts is given in Fig. 3. It can be seen from Fig. 3 that up to a

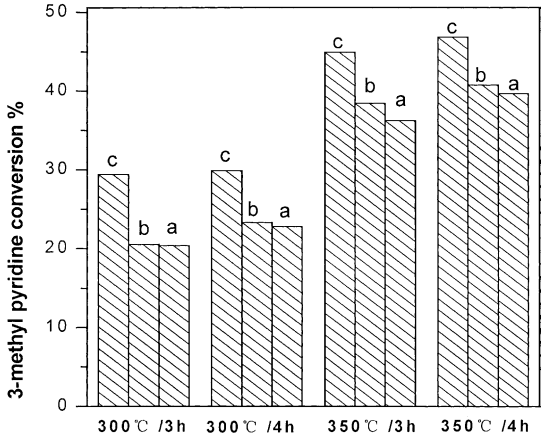

Fig. 3. Effect of reaction temperature and MoO_3 loading ((a) 5 wt.%; (b) 10 wt.%; (c) 15 wt.%) on the conversion of Mo_2N/γ-Al_2O_3 catalysts. Values measured at 3.0 MPa and WHSV = 1.0 h^{-1} for a reactant mixture containing 10% 3-methyl pyridine and 90% methyl cyclohexane.

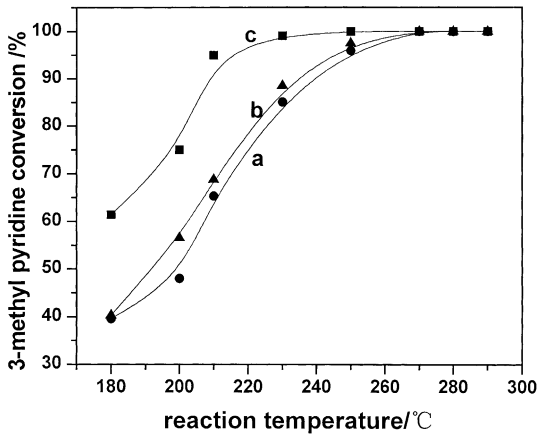

Fig. 4. The conversion and reaction temperature of 3-methyl pyridine HDN over various catalysts: (a) $NiMoN_x/\gamma$-Al_2O_3 (5 wt.%); (b) $NiMoN_x/\gamma$-Al_2O_3 (5 wt.%, 10 wt.%); (c) $NiMoN_x/\gamma$-Al_2O_3 (5 wt.%, 15 wt.%). Conversion measured at 3.0 MPa and WHSV = 1.0 h^{-1} for a reactant mixture containing 10% 3-methyl pyridine and 90% methyl cyclohexane.

temperature of 623 K, the conversion of 3-methyl pyridine increases with increasing temperature. This pattern suggests that, above 573 K, the kinetics become sufficiently rapid to give rise to an increase with increasing temperature for converting the products of the equilibrium reaction to other products in the conversion of 3-methyl pyridine. Moreover, the HDN conversion of Mo_2N/γ-Al_2O_3 increases according to the trend: 5 wt.% < 10 wt.% < 15 wt.% MoO_3 content. This implies that increasing the MoO_3 content in the catalyst just increases the number of the catalytic sites, without changing the nature of the sites.

The temperature dependence of the conversion for 3-methyl pyridine HDN was determined for three catalyst samples, referred to as $NiMoN_x/\gamma$-Al_2O_3 (Fig. 4). As shown in the figure, the conversions of 3-methyl pyridine over all $NiMoN_x/\gamma$-Al_2O_3 catalysts are higher than 97% when the reaction temperature is higher than 523 K. It is clear that the $NiMoN_x/\gamma$-Al_2O_3 catalysts show higher conversion than the Mo_2N/γ-Al_2O_3 catalysts, although both catalysts contained the same amounts of MoO_3. It is well recognized that the addition of Ni to Mo catalysts enhances the conversions of 3-methyl pyridine HDN.

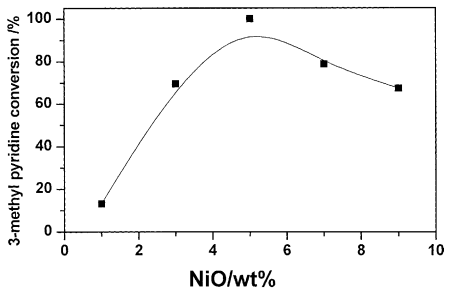

Fig. 5. Effect of the NiO loading on the conversion of $NiMoN_x/\gamma\text{-}Al_2O_3$ catalyst for HDN of 3-methyl pyridine. Conversion measured at 533 K, 3.0 MPa and WHSV = $1.0\,h^{-1}$ for a reactant mixture containing 10% 3-methyl pyridine and 90% methyl cyclohexane.

3.5. The role of Ni in HDN reaction

In order to examine the effect of Ni in $NiMoN_x/\gamma\text{-}Al_2O_3$ catalyst, the specific conversions over these $NiMoN_x/\gamma\text{-}Al_2O_3$ (from 1 to 9 wt.% NiO) catalysts were tested. In this study, the nickel effect was extensively studied with 15.0 wt.% MoO_3 on $\gamma\text{-}Al_2O_3$. Fig. 5 gives the results of nickel promotion on HDN at 563 K. The optimum loading of NiO is found to be around 5.0 wt.% when MoO_3 is about 15 wt.% in $NiMoN_x/\gamma\text{-}Al_2O_3$catalyst. For sulfide catalyst, Ni and Co are the effective promoters that enhance and maintain the catalytic performance of Mo or W. This study confirms that Ni is also an effective promoter in nitride catalyst for HDN reaction.

XRD data shows that metallic Ni is formed in the nitrided $Ni/\gamma\text{-}Al_2O_3$, and no Ni_3N phase emerges. It was reported that Ni_3N would decompose at temperatures higher than 573 K [17]. Therefore, it is probable that nickel is mainly present as metallic Ni in nitrided Ni in this study. The surface atomic concentrations of $NiMoN_x/\gamma\text{-}Al_2O_3$ catalyst passivated and reduced at 673 K are presented in Table 2. It shows that metal Ni emerges on the surface only after reduction by H_2. It is well known that removal of nitride requires hydrogenation first and that metal Ni is active in hydrogenation reaction, so the $NiMoN_x/\gamma\text{-}Al_2O_3$ catalysts possess better HDN property than the other catalysts.

XRD patterns also show that some quantities of Ni_3Mo_3N compound are formed on nitrided $NiMoN_x/\gamma\text{-}Al_2O_3$ with high loading of Ni and Mo. It was reported that the specific activity of Co_3Mo_3N is higher than that of Mo_2N for HDS of thiophene [18]. Therefore, one reason for the high HDN activity of $NiMoN_x/\gamma\text{-}Al_2O_3$ catalyst could be that the Ni_3Mo_3N phase is more active than Mo_2N (or nitrided Ni) for 3-methyl pyridine HDN reactions. Another important reason for the high activity of $NiMoN_x/\gamma\text{-}Al_2O_3$ is the synergy between nitrided Ni and nitrided Mo.

Table 2
Atomic concentration of $NiMoN_x/\gamma\text{-}Al_2O_3$ catalyst

Element	Atomic concentration (%)	
	Passivation	Reduction
N 1s	3.81	2.80
Mo 3d	3.13	2.91
Al 2p	32.71	33.07
O 1s	60.36	60.81
Ni 2p	0.00	0.39

It is concluded that $\gamma\text{-}Al_2O_3$ contains surface sites that preferentially adsorb the molybdate species, which in turn provide adsorption sites for nickel species. Based on this model, both molybdenum and nickel could be well dispersed and hence display high activities. Therefore, a synergy mechanism can be proposed in $NiMoN_x/\gamma\text{-}Al_2O_3$ catalyst. Hydrogen activation mostly takes place on metallic Ni; some activated hydrogen participates directly in the HDN reaction on Ni sites, other activated hydrogen migrates to Mo sites and creates and modifies the catalytic active sites which are also responsible for HDN reaction.

4. Conclusions

1. The XRD measurement shows that $NiMoN_x/\gamma\text{-}Al_2O_3$ is formed as Ni, Mo_2N and Ni_3Mo_3N in the HDN catalyst.
2. TPR experiments indicate that the addition of Ni decreases the reduction temperature of the passivation layer of nitride.
3. Mo 3d spectrum means that there are three state Mo ions on the catalyst surface, i.e. the binding energies 232.3, 229.8 and 228.2 eV are assigned to Mo^{6+}, Mo^{4+} and $Mo^{\delta+}$ ($0 < \delta < 2$), respectively. The atomic ratio of N/Mo, O/Mo and

the content of Mo^{6+} decrease strongly with increasing temperature, while the content of $Mo^{\delta+}$ increases intensively, moreover, there is some oxygen which is difficult to eliminate by reduction by H_2 at a moderate temperature such as 673 K. When the temperature is beyond 573 K, the ratio of N/Mo approaches the lattice value 0.5 and remains unchanged.

4. Mo species is active in the HDN as follows: (all catalysts were supported on γ-Al_2O_3) $NiMoN_x$ (5 wt.%, 15 wt.%) > Mo_2N (15 wt.%) > Mo_2N (10 wt.%) > Mo_2N (5 wt.%).
5. This study confirms that nickel is mainly present as metallic Ni in nitride and is also an effective promoter in nitride catalyst for HDN reaction. The optimum loading of NiO is found to be around 5.0 wt.% when MoO_3 is about 15 wt.% in $NiMoN_x/\gamma$-Al_2O_3 catalyst.

Acknowledgements

We are grateful for the Grant-In-Aid for Scientific Key Foundation of the Ministry of Education, Grant No. 99018 and that of Tianjin Natural Science Foundation, PR China, Grant No. 99380171.

References

[1] S.T. Oyama, Catal. Today 15 (1992) 179.
[2] D.J. Sajkowski, S.T. Oyama, Appl. Catal. A 134 (1996) 339.
[3] H. Abe, A.T. Bell, Catal. Lett. 18 (1993) 1.
[4] J.C. Schlatter, S.T. Oyama, J.E. Metcalfe, J.M. Lambert, Ind. Eng. Chem. Res. 27 (1988) 1648.
[5] A. Raje, S.-J. Liaw, K.V.R. Chary, B.H. Davis, Appl. Catal. A 123 (1995) 229.
[6] C.C. Yu, S. Ramanathan, F. Sherif, S.T. Oyama, J. Phys. Chem. 98 (1994) 13038.
[7] R. Kapoor, S.T. Oyama, J. Solid State Chem. 99 (1992) 303.
[8] C. Yongjun, W. Zhaobin, Y. Shuwu, L. Can, X. Qin, M. Enze, Appl. Catal. A 176 (1999) 17.
[9] W.F. McClune (Ed.), JCPDS Power Difffraction File (Inorganic), 1992.
[10] D.S. Bem, C.P. Gibson, H.-C. zur Loye, Chem. Mater. 5 (1993) 397.
[11] Z. Wei, Q. Xin, P. Grange, B. Delmon, J. Catal. 168 (1997) 176.
[12] C.W. Colling, L.T. Thompson, J. Catal. 146 (1994) 193.
[13] P. Grange, X. Vanhaeren, Catal. Today 36 (1997) 375.
[14] J.G. Choi, D. Choi, L.T. Thompson, Mater. Res. Soc. Extended Abstract EA 24 (1990) 191.
[15] J.G. Choi, J.R. Brenner, C.W. Colling, B.G. Demczyk, J.L. Dunning, L.T. Thompson, Catal. Today 15 (1992) 201.
[16] J. Goldwasser, S.M. Fang, M. Houalla, A.T. Bell, J.A. Reimer, J. Catal. 34 (1995) 104.
[17] M.J.F.M. Verhaak, A.J. Van Dillen, J.W. Geus, Appl. Catal. A 105 (1993) 251.
[18] D.-W. Kim, D.-K. Lee, S.-K. Ihm, Catal. Lett. 43 (1997) 91.